

DD

cea
C.E. SACLAY
DSM

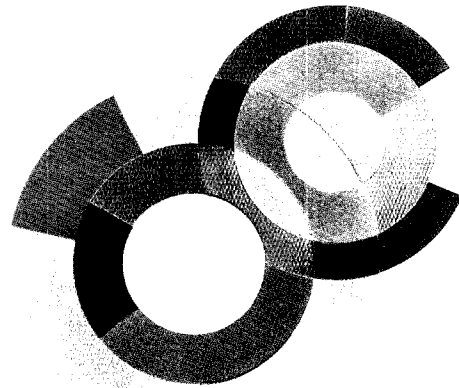
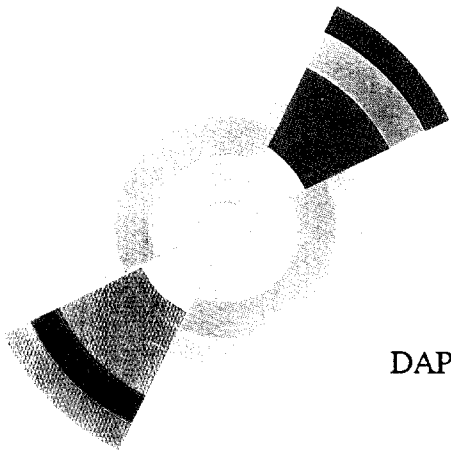
SERVICE DE PHYSIQUE DES PARTICULES



SCAN-9607043

CERN LIBRARIES, GENEVA

SW9637



DAPNIA/SPP 96-13

August 1996

SOME NEW SALIENT FEATURES OF DEEP-INELASTIC SCATTERING AT HERA

J. Feltesse

DAPNIA

*Zeuthen Workshop on Elementary Particle Theory QCD and QED in
Higher Orders, Rheinsberg, Germany,
April 21-26, 1996*

Le DAPNIA (Département d'Astrophysique, de physique des Particules, de physique Nucléaire et de l'Instrumentation Associée) regroupe les activités du Service d'Astrophysique (SAp), du Département de Physique des Particules Élémentaires (DPhPE) et du Département de Physique Nucléaire (DPhN).

Adresse : DAPNIA, Bâtiment 141
CEA Saclay
F - 91191 Gif-sur-Yvette Cedex

Some new salient features of deep-inelastic scattering at HERA

J. Feltesse ^a

^aDSM/DAPNIA/Service de Physique des Particules,
CEA Saclay, F-91191 Gif-sur-Yvette, France

Recent results on deep-inelastic scattering from the H1 and ZEUS collaborations are presented. These include new measurements based on 1994 data together with preliminary results of 1995 data on the structure function F_2 , the gluon density in the proton from analysis of scaling violation, the longitudinal structure function F_L and the structure function $F_2^{c\bar{c}}$. New data on inclusive measurements of diffractive deep-inelastic events and extraction of the debatable Pomeron structure function are also presented.

1. INTRODUCTION

In deep-inelastic lepton-nucleon scattering (DIS) at HERA Q^2 , minus the squared 4-momentum of the exchanged virtual photon, can reach 90000 GeV² and x , the fraction of proton momentum carried by the struck quark can be as low as $5 \cdot 10^{-5}$ at Q^2 values ≤ 4 GeV². The low x and high Q^2 regimes are new domains in which to test QCD.

The large range of DIS data on inclusive and final state distributions at HERA provides a very rich source of information on perturbative QCD and on the transition between perturbative and non-perturbative QCD. In this review we only concentrate on some new salient features. In the second section we present the most recent results on the structure function $F_2(x, Q^2)$ of the proton together with the first determination of the longitudinal structure function $F_L(x, Q^2)$ and of $F_2^{c\bar{c}}$ the charm contribution to the structure function F_2 . The third section is devoted to the most recent findings on the diffractive DIS events, the special class of events where the proton stays almost intact in the collision. We show how the new data can be interpreted in terms of the debatable structure function of the Pomeron.

2. STRUCTURE FUNCTION $F_2(x, Q^2)$

The first determination [1,2] of the proton structure function $F_2(x, Q^2)$ at HERA in 1992 has been based on a recorded luminosity of about 30 nb^{-1} and has revealed the striking feature

of a proton structure function rising as x decreases below 10^{-2} , for Q^2 values in the range $8 < Q^2 < 60$ GeV².

The published 1994 data [3] from the H1 collaboration represents an increase of about a factor 100 in statistics at large Q^2 together with an extension of the accessible kinematic range towards $Q^2 = 1.5$ GeV² and $x = 0.00005$. The preliminary 1995 data [4] from the ZEUS collaboration provide a first glimpse into the $Q^2 < 1$ GeV² region.

At very high $Q^2 \geq 5000$ GeV² the number of recorded events is so far too meager to extract structure functions of neutral or charge currents. Data at high Q^2 are however very sensitive to new phenomena by comparing the measured differential cross section $d\sigma/dQ^2$ with the expected cross section from the standard model, the HERA experiments have provided new limits on masses and couplings of leptoquarks and on fermion compositeness scales [5].

2.1. Scaling violations

The results on $F_2(x, Q^2)$ from H1 1994 data together with those of BCDMS [6], E665 [7] and NMC [8] are shown in fig. 1 as a function of Q^2 at fixed x values. It is striking that in a large part of the kinematical domain at not too small nor too large Q^2 values, the systematics are at present below 5 %. The H1 data agree well with a smooth extrapolation from NMC and BCDMS data. As in the fixed target domain, there are no scaling violations at $x \sim 0.1$, but pronounced Q^2

scaling violations at low x , becoming steeper with x decreasing towards $x = 0.00005$.

The H1 collaboration has made a common fit of the 1994 data at $Q^2 > 5 \text{ GeV}^2$ together with the new NMC data and the BCDMS measurements. The fit is based on Next-To-Leading order (NLO) DGLAP evolution equations. It gives a very good description of the data at $Q^2 > 5 \text{ GeV}^2$ and evolving backwards down to $Q^2 = 1.5 \text{ GeV}^2$ provides a prediction which is also in good agreement with the data (see fig. 1). The fit provides a determination of the gluon density with an accuracy a factor of two better than the previous determinations [9,10]. A steep rise of the gluon density towards low x is observed (fig. 2). The rise is more pronounced when Q^2 increases.

2.2. The x dependence of F_2

Before data from HERA have become available, the x dependence of F_2 was assumed to be of non-perturbative origin and usually taken empirically at an input Q^2 value around 4 GeV^2 . We have seen that the scaling violations provide already crucial information on the rise of the gluon density towards low x . In perturbative QCD the rise of the gluon density should be related to the rise of the sea quark density. The study of the rise of F_2 towards low x is a new insight into perturbative QCD.

The results on $F_2(x, Q^2)$ from H1 (published) [3] and ZEUS (preliminary)[11] are shown in fig. 3 as a function of x at fixed Q^2 values. It is remarkable that the data sets of H1 and ZEUS agree well within the present small errors. It is striking that the steep rise of F_2 with decreasing x persists to Q^2 values as low as 1.5 GeV^2 at $x < 10^{-2}$ and is already visible at $Q^2 = 2000 \text{ GeV}^2$ at $x \sim 0.1$. To quantify the rise of F_2 the H1 collaboration has extracted the average derivative $\langle \frac{d \ln F_2}{d \ln Q^2} \rangle$ by fitting the power λ characterising the rise of $F_2 \propto x^{-\lambda}$ for each Q^2 bin and $x < 0.1$. A rise of λ with $\log Q^2$ is observed from about 0.2 to 0.4 at Q^2 values from 1.5 to 800 GeV^2 (fig. 4).

At sufficiently low x values, in perturbative calculations resummations based on leading $(\alpha_s \log(Q^2/Q_0^2))^n$ terms, the so-called Dokshitzer Gribov Lipatov Altarelli Parisi (DGLAP) mechanism [12] should eventually be superseded

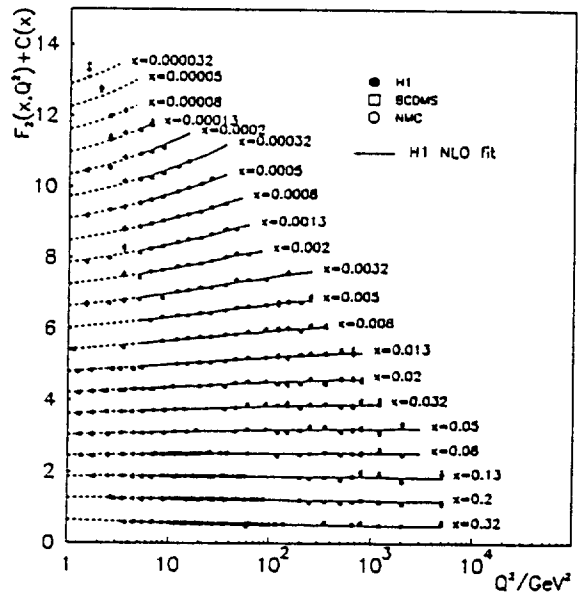


Figure 1. The proton structure function $F_2(x, Q^2)$ vs Q^2 for fixed values of x . The 1994 data from H1 (closed points) are compared to the fixed target data of BCDMS (open triangles) and NMC (open circles). The full lines represent the DGLAP NLO QCD fit using data at $Q^2 > 5 \text{ GeV}^2$. The dashed line represent the backward extension of the fit. For clarity the F_2 values are plotted adding a term $c(x) = 0.6(i_x - 0.4)$ to F_2 , where i_x is the bin number starting at $i_x = 1$ for $x = 0.32$.

by resummations based on leading $(\alpha_s \log 1/x)^n$ terms, the so-called Balitski Fadin Kuraev Lipatov (BFKL) mechanism [13].

It is tempting to attribute the rise of F_2 to the BFKL mechanism where an even steeper power $\lambda = 0.5$ is predicted at leading order. The predicted value is higher than the data but there is indication that the effective power should be a bit smaller when calculated more accurately at NLO [14] or in the frame of the BFKL inspired dipole model [15]. We should however not forget that at low x and high Q^2 , independent of any BFKL mechanism, it has been predicted a long time ago

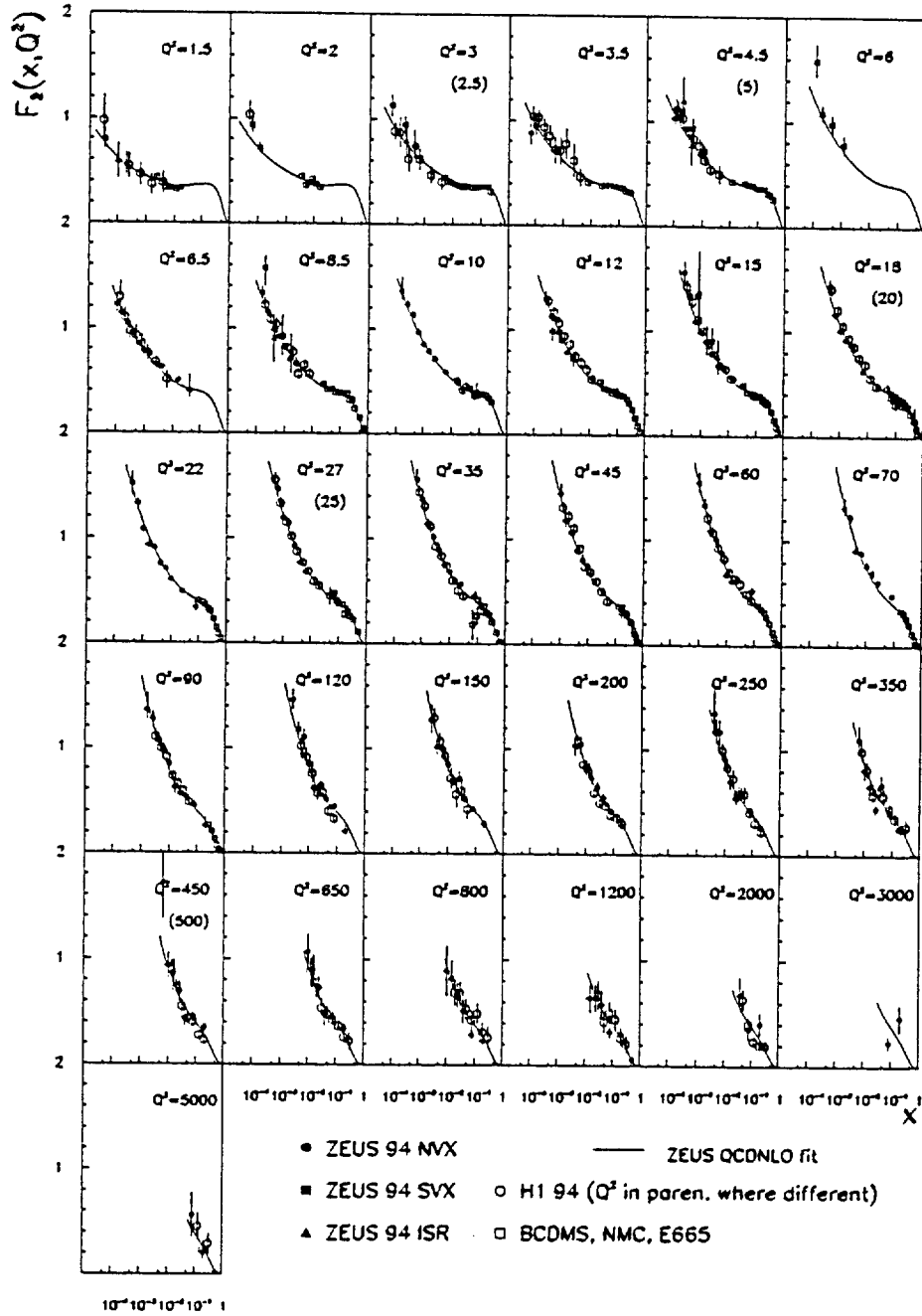


Figure 3. The proton structure function F_2 . The 1994 data from H1 and ZEUS with Nominal Vertex (NVX), Shifted Vertex (SVX) and Initial State Radiation (ISR). The HERA data are compared to the fixed target data of BCDMS, NMC and E665. The full line represents the DGLAP NLO fit of all the ZEUS data points combined with the NMC data at $Q^2 > 4 \text{ GeV}^2$.

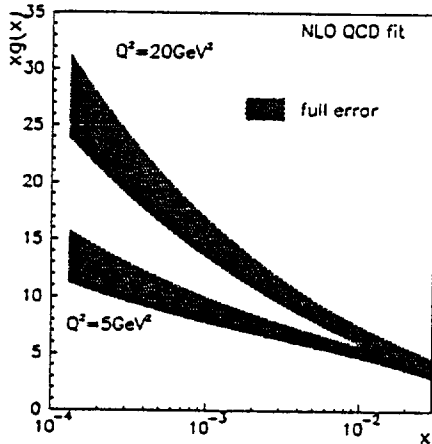


Figure 2. The gluon density $xg(x)$ at $Q^2 = 5 \text{ GeV}^2$ and $Q^2 = 20 \text{ GeV}^2$ extracted from a NLO QCD fit combining H1 1994 with NMC and BCDMS F_2 data. The band represents the full experimental errors.

[16] that the proton structure function F_2 should rise at low x and that the growth should increase with increasing Q^2 provided F_2 is non singular at some low Q^2 boundary value. The prediction is an intrinsic property of QCD as a non-abelian asymptotically free field theory. It has moreover been predicted that the growth should be weaker than a power law in $\frac{1}{x}$ but more rapid than any power of $\log \frac{1}{x}$. This part of the prediction is an apparent contradiction with the $x^{-\lambda}$ behaviour of the data. However the measured power λ is not the result of a fit of F_2 but an average derivative in the accessed range in x which varies with Q^2 .

The data can be equally well described in each bin of Q^2 by an x dependence in $\exp \sqrt{\ln \frac{1}{x}}$ [3,17], as predicted in the double leading log ($\log(Q^2) \log \frac{1}{x}$) approximation [18], or by global fits based on the dipole BFKL mechanism [15] or by a sum of singlet and non-singlet parametrizations where the power λ is independent of Q^2 at $Q^2 > 10 \text{ GeV}^2$ [19]. To get more insight into the underlying QCD mechanism requires probably measurements other than F_2 , such as the longitudinal structure function F_L and the properties of the hadronic final state.

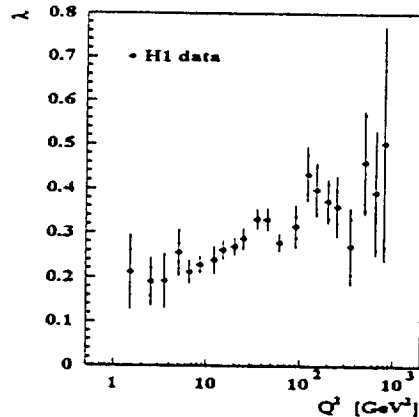


Figure 4. The exponent λ from fits of the form $F_2 \propto x^{-\lambda}$ of the measured structure function F_2 from the H1 experiment at fixed Q^2 values and for $x < 0.1$

2.3. $F_2(x, Q^2)$ at very low Q^2

At low Q^2 in the transition region between photoproduction and DIS there are two types of approach to generate the shape of the structure function :

- a model [20] where all parton densities are generated from intrinsic non-perturbative valence-like distributions at some low scale μ . The observed rise of F_2 at low x is generated by the perturbative QCD evolution starting at $\mu = 0.3 \text{ GeV}^2$. This model has been so far very successful in predicting HERA data at low x and $Q^2 > 1.5 \text{ GeV}^2$ [3].
- models based on Regge theory which provide an economical parametrization of all hadron-hadron total cross sections. In these models [21,22] the evolution at low Q^2 of F_2 is generated by empirical simple functions of Q^2 that vanish linearly with Q^2 as $Q^2 \rightarrow 0$. The Regge inspired models lie below the data at $Q^2 > 2 \text{ GeV}^2$.

In 1995 the ZEUS collaboration [4] has added a small calorimeter close to the beam axis and obtained data at $0.15 < Q^2 < 0.6 \text{ GeV}^2$. The preliminary results based on 1/4 of the statistics

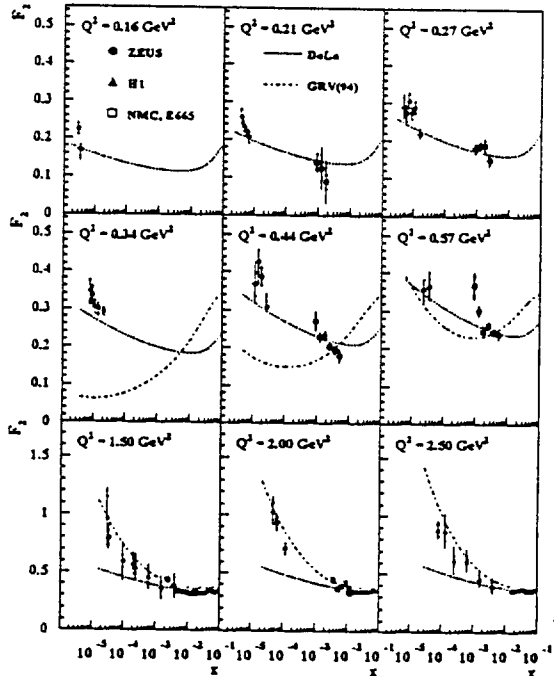


Figure 5. The low Q^2 structure function F_2 vs x . The data points of ZEUS, H1, NMC and E665 are compared to the predictions of the DL Regge model and of the GRV parametrization.

are shown on fig. 5. The data are in reasonable agreement with the Regge inspired parametrization DL [21] and in clear disagreement with the GRV parametrization at $Q^2 < 0.5 \text{ GeV}^2$.

2.4. Structure function $F_L(x, Q^2)$

At $Q^2 < 1000 \text{ GeV}^2$, the inclusive differential cross section $\frac{d^2\sigma}{dydQ^2}$ depends actually on two structure functions: $F_2(x, Q^2)$ and the longitudinal structure function $F_L(x, Q^2)$:

$$\frac{d^2\sigma}{dydQ^2} = \frac{2\pi\alpha^2}{Q^4y} [(1 + (1 - y)^2) F_2(x, Q^2) - y^2 F_L] \quad (1)$$

The contribution of F_L is negligible at low y but assumptions on F_L values must be made at large y to extract F_2 from the measurement. There are also numerous old [23] and recent QCD predictions which relate F_L to the gluon and quark densities in the proton [24,15,19].

The usual method to measure F_L is to measure the differential cross section at fixed (Q^2, x)

bins but different y values by running at different beam energy settings. The H1 collaboration has proposed recently another method. The structure function F_2 is extracted from the differential cross section at low y , a domain where F_L hardly contributes. Then at larger y , the value of F_2 is extrapolated with the DGLAP evolution equation. Finally from the measurement at large y together with the extrapolated value of F_2 the structure function F_L is extracted from the equation (1) in bins of x . In contrast to the usual method it has to be assumed that we can use the DGLAP evolution equations to predict the values of F_2 at $Q^2 > 8 \text{ GeV}^2$ and $x > 10^{-4}$ using as input values the result of the NLO fit of data at $Q^2 > 4 \text{ GeV}^2$ and at $y < 0.35$. This assumption is reasonable because the HERA data so far have shown that the DGLAP evolution equations are still valid in this domain independently of the value of F_L . The resulting value based on a luminosity of 1.25 pb^{-1} is shown in fig. 6. Within the errors, the F_L values are consistent with the value of about 0.4 which can be inferred from perturbative QCD based on the DGLAP mechanism [23] and using the gluon density extracted from scaling violations.

2.5. Structure function F_2^{cc}

At HERA, in a sample of DIS events the H1 collaboration has observed nice signals of D^0 and D^* from the reconstruction of tracks of the hadronic final state [25]. For a recorded luminosity of 3 pb^{-1} H1 has obtained $104 \pm 12 D^*$ events and $144 \pm 19 D^0$ events in the rapidity range $|\eta| < 1.5$. at $10 < Q^2 < 100 \text{ GeV}^2$. Assuming charm tagging efficiencies $P(c \rightarrow D^0) \cdot BR(D^0 \rightarrow K^-\pi^+) = 0.02$, $P(c \rightarrow D^*) \cdot BR(D^* \rightarrow D^0\pi^+) \cdot BR(D^0 \rightarrow K^-\pi^+) = 0.007$, the signal has been converted into a charm cross section in each (Q^2, x) bin. The charm contribution F_2^{cc} to the proton structure function has been extracted after neglecting the F_L contribution at $y < 0.5$. The results are shown on fig.7 and compared to NLO calculations [26] using the GRV-HO [20] and CTEQ2MF[27] parametrizations of the gluon density. The agreement between NLO QCD calculations and the data is remarkable for this very first measurement of F_2^{cc} at low x values.

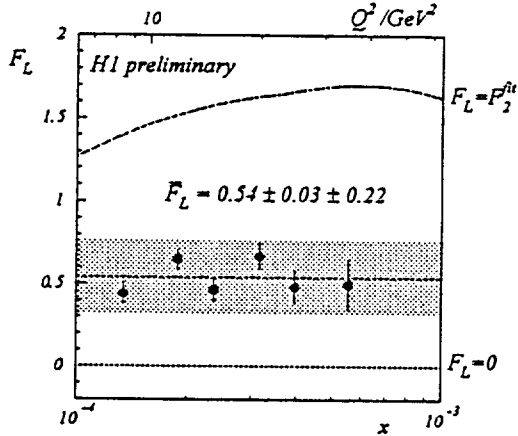


Figure 6. The preliminary determination of the longitudinal structure function F_L by the H1 collaboration. The errors bars of the data are statistical. The grey band shows the size of the correlated systematic errors around the average value.

3. Diffractive deep-inelastic scattering

It was anticipated that the HERA collider should provide a rather unique possibility to study diffractive dissociation at short distances [23] and that the rapidity gap would be a powerful criterion to select diffractive deep-inelastic events as shown in fig. 8 [29]. Analysing the 1992 data, the ZEUS and H1 collaborations [30,31] have reported observation of deep-inelastic events in which no energy flow is observed in a large region of rapidity close to the proton direction (fig. 8).

Independently of any assumption on the diffraction mechanism two variables can be defined :

$$x_P = \frac{Q^2 + M_X^2}{Q^2 + W^2} \quad (2)$$

$$\beta = \frac{Q^2}{Q^2 + M_X^2} \quad (3)$$

where M_X^2 and W^2 are the squared invariant masses of the hadronic system X and of the total hadronic system ($X + Y$) respectively. The variables β and x_P are trivially related to x the usual

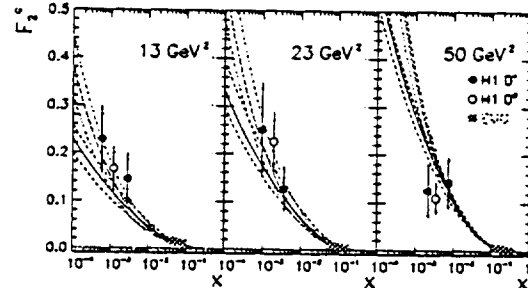


Figure 7. The charm contribution $F_2^{c,c}$ to the proton structure function as derived from the inclusive D^{*+} and D^0 preliminary analysis from the H1 collaboration. Data are compared with NLO calculations based on GRV (upper lines) and CTEQ2MF (lower lines) with $m_c = 1.5$ GeV. The dashed lines give predictions for $m_c = 1.3$ GeV and $m_c = 1.7$ GeV. The EMC data is also shown.

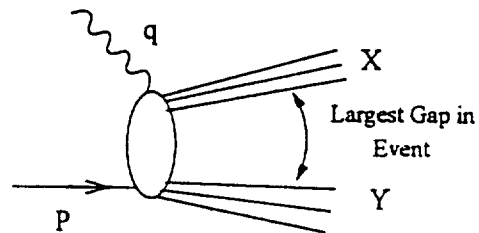


Figure 8. Basic Feynman diagram for diffractive deep-inelastic events.

Bjorken variable in DIS by

$$x = \beta x_P. \quad (4)$$

In a model where diffraction in DIS is produced by a Pomeron with a partonic structure [32], x_P is the fraction of the proton energy carried by the Pomeron and β is the fraction of the Pomeron energy carried by the parton which interacts with the virtual photon.

3.1. Structure function $F_2^{D(3)}(x_P, \beta, Q^2)$

In analogy to the proton structure function $F_2(x, Q^2)$ it is possible to define a 3-variable

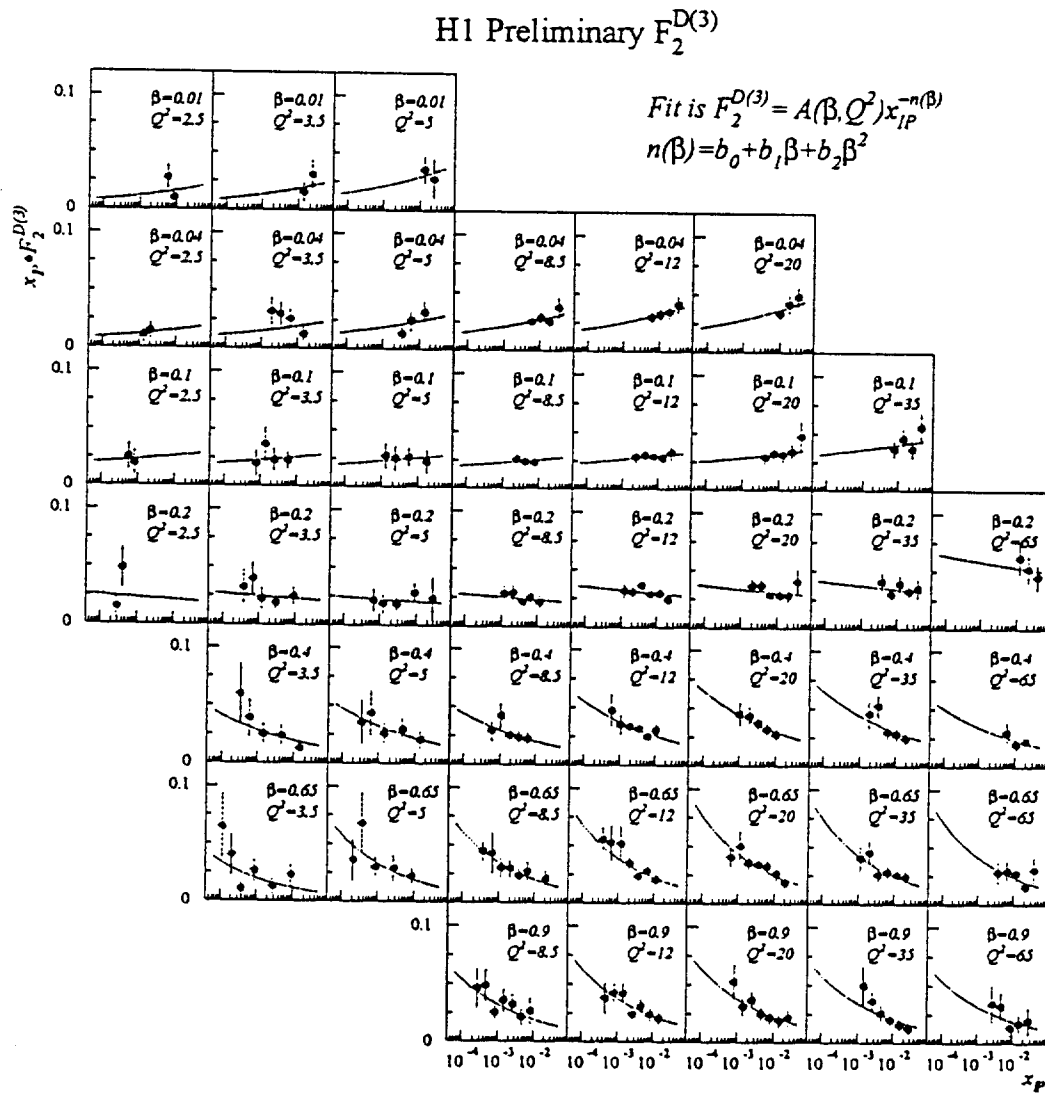


Figure 10. The 1994 diffractive contribution $F_2^{D(3)}(x_p, \beta, Q^2)$ to the proton structure function F_2 as a function of x_p for different β and Q^2 measured by the H1 collaboration. For clarity each data point is multiplied by x_p . Superimposed is the result of a fit establishing a breaking of factorization of the flux factor (see text).

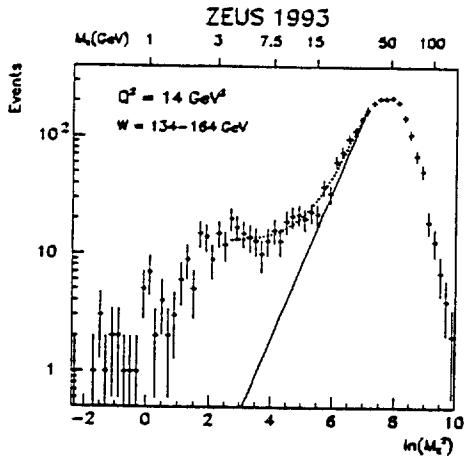


Figure 9. Example of the determination of the non-diffractive background by the ZEUS collaboration. The error bars of the data distribution of $\ln M_X^2$ are statistical. The solid line shows the non-diffractive background as determined by the fit of the data.

structure function $F_2^{D(3)}$ from the cross section

$$\frac{d^3\sigma^D}{dx_{\mathcal{P}}d\beta dQ^2} = \frac{2\pi\alpha^2}{Q^4\beta} \left[(1 + (1-y)^2) F_2^{D(3)}(x_{\mathcal{P}}, \beta, Q^2) \right] \quad (5)$$

where the longitudinal structure function has been set to $F_L = 0$ and where the cross section has been averaged over t the squared 4-momentum transfer at the incident proton vertex. In models with partonic structure of the Pomeron, the structure function $F_2^{D(3)}(x_{\mathcal{P}}, \beta, Q^2)$ should factorize into a Pomeron flux factor $f(x_{\mathcal{P}})$ and a Pomeron structure function $F_2^{D(2)}(\beta, Q^2)$:

$$F_2^{D(3)}(x_{\mathcal{P}}, \beta, Q^2) = f(x_{\mathcal{P}}) F_2^{D(2)}(\beta, Q^2) \quad (6)$$

The early measurements on 1993 data from the H1 (0.3 pb^{-1}) [33] and ZEUS (0.5 pb^{-1}) [34] experiments have indeed yielded a flux term $\propto x_{\mathcal{P}}^{-n}$ which does not depend on β and Q^2 . The two measurements are based on events selected by either a lack of activity in the forward detectors (H1) or by a large rapidity gap (ZEUS). The measured flux factors are perfectly consistent between the two experiments (table 1).

An analysis [35] of the same 1993 data by the ZEUS collaboration but where the diffrac-

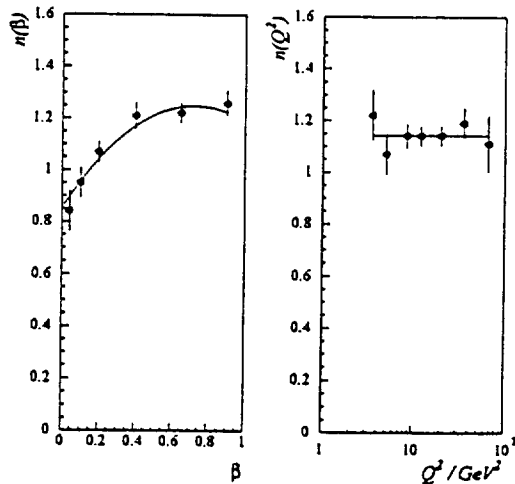


Figure 11. Preliminary result of a determination of the exponent n of the flux factor $x_{\mathcal{P}}^{-n(\beta, Q^2)}$ as fitted in each β or Q^2 interval of the measured $F_2^{D(3)}(x_{\mathcal{P}}, \beta, Q^2)$ by the H1 collaboration. Superimposed is the quadratic fit $n(\beta) = b_0 + b_1\beta + b_2\beta^2$.

tive cross section is inferred from a subtraction of an extrapolation at low M_X of the standard DIS events (see fig. 9) has yielded a higher value of n at three sigmas from the H1 value (table 1). This method is by definition mainly sensitive to low M_X events.

A recent measurement by the ZEUS collaboration of 1994 data based on events where the leading proton has been tagged [36] with $x_L = 1 - x_{\mathcal{P}} > 0.97$ also yields a flux term for $0.07 < \beta < 0.375$ in accord with the two early measurements of H1 and ZEUS (table 1).

Based on a luminosity of 2 pb^{-1} of good data recorded in 1994, the H1 collaboration has obtained a much more precise determination of the structure function $F_2^{D(3)}$ [37]. The results are shown on fig. 10. For clarity, each measured value is multiplied by $x_{\mathcal{P}}$. There is clearly a breaking of factorization. The flux factor is constant with Q^2 but varies with β . The flux power term can be parametrized as

$$n(\beta) = b_0 + b_1\beta + b_2\beta^2. \quad (7)$$

Table 1
Flux power term in diffractive DIS event $d\sigma/dx_P \propto x_P^{-n}$

data sources	n	selection of events
H1 93 [33]	$1.19 \pm 0.06 \pm 0.07$	forward detectors
ZEUS 93,1 [34]	$1.30 \pm 0.08^{+0.08}_{-0.14}$	rapidity gaps
ZEUS 93,2 [35]	$1.46 \pm 0.04 \pm 0.08$	low M_X extrapolation
ZEUS 94 [36]	$1.28 \pm 0.07 \pm 0.15$	leading proton tagging
H1 94 [37]	from 0.8 to 1.3	forward detectors, n varies with β or M_X

The result of the fit is superimposed on fig. 10 and shown as a function of β or Q^2 in fig. 11. The increase of n with increasing β (or equivalently with decreasing M_X) has been used as a possible explanation for the spread of the 1993 data (table 1). This is at present clearly demonstrated by the new H1 data and is a challenge for all theoretical interpretations of the diffractive DIS events at HERA.

3.2. Structure function

To investigate the Q^2 and β behaviour of $F_2^{D(3)}(x_P, \beta, Q^2)$ it is convenient to define

$$\bar{F}_2^D(\beta, Q^2) = \int_{x_{P_1}}^{x_{P_h}} F_2^{D(3)}(x_P, \beta, Q^2) dx_P \quad (8)$$

where the integration limits $x_{P_1} = 0.003$ and $x_{P_h} = 0.05$ have values chosen to be near the experimentally accessed range. In a naive factorisation model with exchange of a Pomeron, $\bar{F}_2^D(\beta, Q^2)$ would be simply proportional to the structure function of the Pomeron. More generally, \bar{F}_2^D amounts to the structure function of the hadronic exchange averaged over a wide range in x_P and t .

The result of the integral of the structure function $F_2^{D(3)}(x_P, \beta, Q^2)$ over x_P measured by the H1 collaboration is shown on fig. 12. The structure function $\bar{F}_2^D(\beta, Q^2)$ is almost constant with β but has strong scaling violations which persist to $\beta = 0.65$ as a rise in Q^2 . If the scaling violation are interpreted as a putative partonic structure of \bar{F}_2^D which satisfies the DGLAP evolution equation, one obtains the striking result that at $Q^2 = 5 \text{ GeV}^2$ the input parton distribution should be mainly gluonic with a gluon density peaking close to $\beta = 1$ (see fig. 13). This is consistent with a study of the hadronic final

state in diffractive DIS events [39]. Evidence for a 'leading' gluon structure of the Pomeron has also been inferred from a combined analysis of jet production in diffractive photoproduction and of $F_2^{D(3)}$ with no taken into account of Q^2 evolution [38].

4. CONCLUSION

By spring 1995, most of the final results of the analysis of the 1994 data at HERA based on 3 to 5 pb⁻¹ of good recorded data by the H1 and ZEUS experiments have been produced together with the first preliminary results from 1995 data. Precision measurements of the proton structure function F_2 at moderate Q^2 and first hints from the low Q^2 domain allow thorough investigation on the evolution with Q^2 of the x dependence of F_2 . First results on F_L , the longitudinal structure function and on $F_2^{c\bar{c}}$, the charm contribution to F_2 have been reported. In diffractive DIS events a clear breaking of factorization has been observed. These beautiful results represent however only a small part of the physics message from HERA. Many other topics such as studies of the final states in DIS, α_s measurement, photoproduction, heavy quark and vector meson production, searches beyond the standard model have been omitted. The two experiments have each recorded an other 5 pb⁻¹ of data in 1995 and ten to hundred times more luminosity are still to be produced in the coming years. HERA physics has just started but with a flourish.

5. Acknowledgements

It is a pleasure to thank all my colleagues from ZEUS and H1 for providing me with their data.

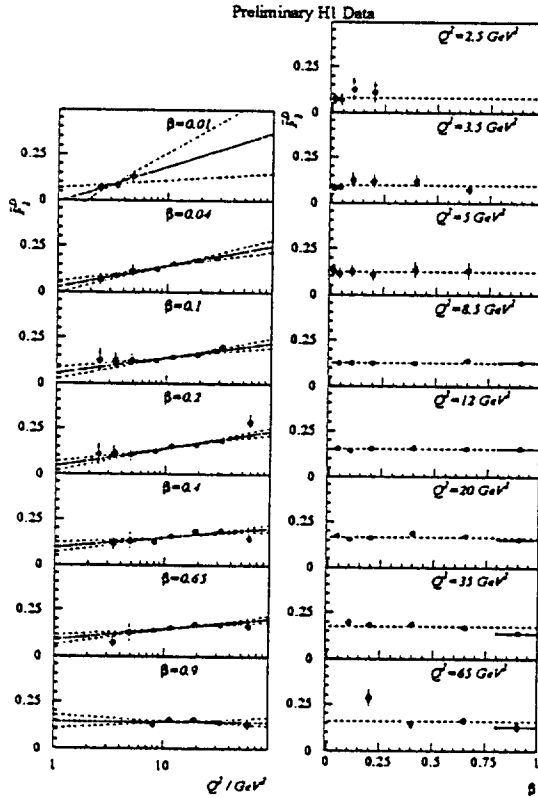


Figure 12. The structure function $\tilde{F}_2^D(\beta, Q^2)$ measured by the H1 collaboration. Superimposed are the results of fits which assume leading logarithm scaling violations. The best fit (continuous curve) and the curves corresponding to a change of ± 1 sigmas (dashed curves) are shown.

I thank specially G. Cozzika and J. Dainton for help in preparing the manuscript.

REFERENCES

1. H1 Collaboration, I. Abt et al., Nucl. Phys. B407 (1993) 515.
2. ZEUS Collaboration, M. Derrick et al., Phys. Lett. B316 (1993) 412.
3. H1 Collaboration, S. Aid et al., preprint DESY 96-039.
4. ZEUS Collaboration, R. Yoshida and Q. Zhu,

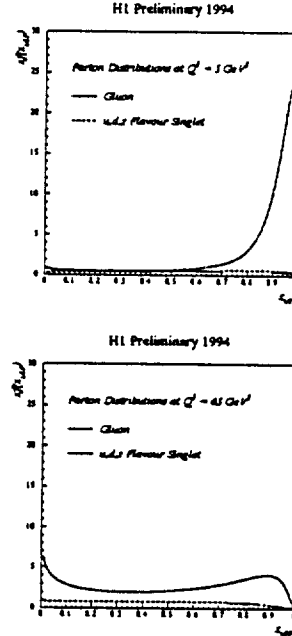


Figure 13. Parton distributions used as input values at $Q^2 = 5 \text{ GeV}^2$ to the leading logarithm fits of $\tilde{F}_2^D(\beta, Q^2)$ from the H1 experiment. Also shown are the parton distributions after evolution to $Q^2 = 65 \text{ GeV}^2$.

Proc. of the International Workshop on Deep Inelastic Scattering and Related Phenomena, Roma (Italy), April 1996.

5. H1 Collaboration, S. Aid et al., Phys. Lett. B353 (1995) 578.
6. BCDMS Collaboration, A.C. Benvenuti et al., Phys. Lett. B223 (1989) 485.
7. E-665 FNAL Collaboration, M.R. Adams et al., FNAL-Pub-95/396-E (1995).
8. NMC Collaboration, M. Arneodo et al., Phys. Lett. B364 (1995) 107.
9. H1 Collaboration, S. Aid et al., Phys. Lett. B354 (1995) 494.
10. ZEUS Collaboration, M. Derrick et al., Phys. Lett. B345 (1995) 576.
11. ZEUS Collaboration, M. Derrick et al., Zeit. Phys. C69 (1996) 607 and R. Yoshida, Proc. of the International Workshop on Deep Inelastic Scattering and Related Phenomena,

- Roma (Italy), Apr. 1996.
12. V.N. Gribov and L.N. Lipatov, *Sov. J. Nucl. Phys.* 15 (1972) 438 and 675;
G. Altarelli and G. Parisi, *Nucl. Phys.* B126 (1977) 298 ;
Yu.L. Dokshitzer, *Sov. Phys. JETP* 46 (1977) 641.
 13. E.A. Kuraev, L.N. Lipatov and V.S. Fadin, *Phys.Lett.* B60 (1975) 50 ;
Ya.Ya. Balitski and L.N. Lipatov, *Sov. J. Nucl. Phys.* 28 (1978) 822 and *Zh. Eksperiment. I. Teor.Fiz.* 72 (1977) 377.
 14. R.E. Hancock and D.A. Ross, *Nucl. Phys.* B383 (1992) 575;
J.C. Collins and P.V. Landshoff, *Phys. Lett.* B276 (1992) 196;
R. Peschanski and S. Wallon, *Phys. Lett.* B349 (1995) 357;
A.H. Mueller, *Nucl. Phys.* B415 (1994) 373;
A.J. Askew et al., *Phys. Rev.* D49 (1994) 4402;
V.S. Fadin and L.N. Lipatov, *Proc. of the Topical Conference on Hard Diffractive Processes, Eilat (Israel), Feb. 1996*, p.572.
 15. H. Navelet et al., *Preprint DESY 96-108 and Saclay DAPNIA/SPP 96-08*, hep-ph/9605/389.
 16. A. De Rújula et al., *Phys. Rev.* D10 (1974) 1649.
 17. A. De Roeck, M. Klein and T. Naumann, *preprint DESY 96-063*.
 18. R.D. Ball and S. Forte, *Phys. Lett.* B335 (1994) 77.
 19. C. López, F. Barreiro and F.J. Ynduráin, *preprint DESY 96-087*.
 20. M. Glück, E. Reya and A. Vogt, *Zeit. Phys.* C67 (1995) 433.
 21. A. Donnachie and P.V. Landshoff, *Zeit. Phys.* C61 (1994) 139.
 22. A. Capella et al., *Phys. Lett.* B337 (1994) 358.
 23. G. Altarelli and G. Martinelli, *Phys. Lett.* B76 (1978) 89.
 24. B. Badelek, J. Kwieciński and A. Staśto, *preprint Durham DTP 96/16*.
 25. H1 Collaboration, M. Klein, *Proc. of the International Workshop on Deep Inelastic Scattering and Related Phenomena, Roma (Italy), Apr. 1996*.
 26. S. Riemersma, J. Smith and W.L. van Neerven, *Phys. Lett.* B347 (1995) 143.
 27. CTEQ Collaboration, J. Botts et al., *Phys. Lett.* B304 (1993) 15.
 28. R.P. Feynman, 'Photon Hadron Interactions', W. Benjamin Inc., 1972 p. 344. ; J.D. Bjorken in *Proc. on Deep Inelastic Scattering and Related topics, Eilat (Israel), 1994*, p. 151 and earlier references therein.
 29. M.G. Ryskin and M. Besançon, *Proc. Workshop on Physics at HERA (DESY,1991)* p.215 and earlier references therein.
 30. ZEUS Collaboration, M. Derrick et al., *Phys. Lett.* B315 (1993) 481.
 31. H1 Collaboration, T. Ahmed et al., *Nucl. Phys.* B429 (1994) 477.
 32. G. Ingelman and P. Schlein, *Phys. Lett.* B152 (1985) 256.
 33. H1 Collaboration, T. Ahmed et al., *Phys. Lett.* B348 (1995) 681.
 34. ZEUS Collaboration, M. Derrick et al., *Zeit. Phys.* C68 (1995) 569.
 35. ZEUS Collaboration, M. Derrick et al., *Zeit. Phys.* C70 (1996) 391.
 36. ZEUS Collaboration, R. Yoshida, E. Barberis, *Proc. of the International Workshop on Deep Inelastic Scattering and Related Phenomena, Roma (Italy), Apr. 1996*.
 37. H1 Collaboration, A. Mehta, *Proc. of the Topical Conference on Hard Diffractive Processes, Eilat (Israel), Feb. 1996*, p.710.
 38. ZEUS Collaboration, M. Derrick et al., *Phys. Lett.* B356 (1995) 129.
 39. H1 Collaboration, G. Knies, *Proc. of the Topical Conference on Hard Diffractive Processes, Eilat (Israel), Feb. 1996*, p.689.

